Phonon transmission of vacancy disordered armchair silicene nanoribbon

Ashraful Hossain Howlader[1,2,3]*, Md. Sherajul Islam[2], and Naim Ferdous[2,3]

1. School of Physics, The University of Sydney, New South Wales 2006, Australia

2. Department of Electrical and Electronic Engineering, Khulna University of Engineering and Technology, Khulna 9203, Bangladesh

3. Department of Electrical and Electronic Engineering, Bangabandhu Sheikh Mujibur Rahman Science and Technology University, Gopalganj 8100, Bangladesh

(Received 22 November 2020; Revised 23 December 2020)

This work demonstrates the atomic vacancy effects on the phonon properties of armchair silicene nanoribbon in a step by step process for the first time. The phonon localization effect figures out the fact that vacancies cause to high-energy phonons become localized, whereas low-energy phonons can easily transmit. The vacancy reduces high-energy phonon transmission severely compared to low-energy phonon. It is also found from phonon density of states that high-frequency phonons soften towards the low-frequency region. The simulated phonon bandstructure verifies that most of the phonon branches transform to a nondegenerate state from a degenerate state and shifted toward a lower frequency regime due to the presence of vacancies. The overall consequences of atomic vacancies on the phonon thermal conductance disclose the reality that only a few atomic vacancies result in a vital reduction of phonon thermal conductance. In addition, the entropy of the disordered system is investigated.

Document code: A **Article ID:** 1673-1905(2021)08-0454-5

DOI https://doi.org/10.1007/s11801-021-0187-2

Low dimensional nanomaterials are showing their potentialities in the field of nanoelectronics. Among them, silicon's (Si) low dimensional allotropes are getting more research interests due to their potential possibilities in future nanoelectronic devices for compatibility with conventional Si-based electronic technology. Silicene has recently come into the limelight as an alternative to graphene. However, silicene offers semimetallic properties without a significant bandgap similar to graphene. Therefore, opening a bandgap in a silicene sheet is mandatory in implementing promising nanoelectronic devices. One approach is to open a bandgap in silicene through the quantum confinement of carriers by forming nanoribbon structures.

Just like graphene nanoribbons (GNRs), the electrical[1], magnetical[2], optical, thermal[3], and mechanical[4] characteristics of silicene nanoribbons (SiNR) are determined by the structural size and chirality. Armchair edge silicene nanoribbons (ASiNRs) are semiconducting and nonmagnetic on the other hand the zigzag edge silicene nanoribbons (ZSiNRs) are metallic and antiferromagnetic in nature. The unusual and rare sp^2/sp^3 hybridization of SiNR provides some unique physical properties. Angle-resolved photoemission spectroscopy proved that quasiparticles at room temperature behave as massless relativistic Dirac fermions in silicene nanoribbon because of its cone-like dispersion of π and π^* bands around the Fermi level. This would lead to quite high Fermi velocity of $\sim 1.3\times10^6$ ms^{-1} and very promising for forthcoming applications[5]. SiNRs also have a tunable bandgap depending on the size and geometry. Under a transverse electric field, ZSiNR turns into half-metallic and could be used as an effective spin field-effect transistor[6]. High-performance field-effect transistors could be constructed using ASiNR as channel and ZSiNR as electrodes[7]. The tunnel field-effect transistor could also be developed by SiNR[8].

The group led by Aufray et al[9] was the first to produce SiNR on a silver substrate by epitaxial growth. Another group of Tchalala et al[10] developed SiNR on a gold substrate by evaporating Si with direct current heating of a piece of Si wafer. During the growth and implementation of real devices using SiNR, defects like atomic vacancies are not avoidable. Moreover, defects can be engineered to develop the device performance[11].

Many theoretical analyses have been done on the electrical properties of SiNR[12-20]. However, up to now, the analyses on the thermal properties of SiNR are rare. Phonon is the quantized unit of atomic vibration. Phonons are strongly coupled with an electron in low dimensional Si nanomaterials[21]. Therefore, to understand electronic transport properties in those nanomaterials more deeply, the investigation of phonon properties is mandatory.

As far as it is known to the authors, there is no literature on phonon characteristics of SiNR. Here we are

* E-mail: ashraful.howlader@sydney.edu.au

interested to go through a well-arranged theoretical inquiry on phonon properties of ASiNR. Our investigation is not only on pristine ASiNR but also with atomic vacancies. The quantum transport of phonons, phonon localization phenomena, phonon transmission for the whole energy range, phonon density of states (PDOSs), phonon dispersion relation within the whole Brillouin zone, and entropy of pristine as well as vacancy disordered ASiNR are tried to explore with first-principle calculations.

SiNR has a buckled plane, unlike a flat plane of GNR. According to Cahangirov et al[22], the stable silicene sheet is buckled but not planar, because of the tendency of silicon atoms to form bonds mixture of sp^2/sp^3 hybridization instead of only sp^2 hybridization. Here the bond length between two Si atoms is taken as 2.24 Å. The buckling between Si-Si bonds is taken about 0.44 Å for the energetically most favorable and stable condition. A total of 200 Si atoms in 10 ASiNR are taken as a sample to carry out computer simulation. Fig.1(a) shows the low buckled atomic structure of SiNR and Fig.1(b) shows 10 ASiNR.

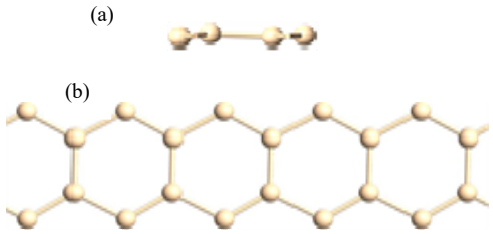

Fig.1 (a) Low buckling of SiNR (side view) and (b) 10 ASiNR (top view)

All the simulations are performed in the Virtual NanoLab software package. The analytical bond-order potentials used here were reported by Erhart et al[23]. The potentials can be calculated in the following way. The cohesive energy is expressed as

$$E=\sum_{i>j} f_{\mathrm{c}}[(r_{ij})-\overline{b}_{ij}V_{\mathrm{A}}(r_{ij})]. \tag{1}$$

The repulsive and attractive factors are expressed as

$$V_{\mathrm{R}}(r)=(D_0/(S-1))\exp[-\beta\sqrt{2S}(r-r_0)], \tag{2}$$

$$V_{\mathrm{A}}(r)=(SD_0/(S-1))\exp[-\beta\sqrt{2S}(r-r_0)], \tag{3}$$

where D_0 and r_0 stand as dimer energy and bond length, respectively, β generates from the ground-state vibrational frequency of the dimer, and S is adjusted to the slope of the Pauling plot. The cutoff function is

$$f_{\mathrm{c}}(r)=\begin{cases}1, & r<R-D\\ \dfrac{1}{2}-\dfrac{1}{2}\sin(\pi/2\dfrac{r-R}{D}), & |R-r|\le D\\ 0, & R+D<r\end{cases}, \tag{4}$$

where R and D represent the position and the width of the cutoff region. The bond-order is

$$b_{ij}=(1+\chi_{ij})^{-1/2}, \tag{5}$$

$$\chi_{ij}=\sum_{k(\neq i,j)} f_{\mathrm{c}}(r_{ik})\exp[2\mu(r_{ij}-r_{ik})]g(\theta_{ijk}), \tag{6}$$

$$g(\theta)=\gamma(1+\frac{c^2}{d^2}-\frac{c^2}{d^2+[h+\cos\theta]^2}), \tag{7}$$

where 2μ, γ, c, d, and h are three-body interactions and depends on the type of atoms i and j.

The geometry of ASiNR is optimized using force tolerance as 0.001 eV/Å and stress tolerance as 0.000 1 eV/Å. Lattice constraints are considered along the x and y-vectors directions. Here the limited memory Broyden Fletcher Goldfarb Shanno optimizer method is employed with a maximum 200 number of steps. The dynamical matrix is obtained with respect to real space displacements of the basis by the harmonic approximation through the central finite difference method. The Brillouin zone is sampled by Monkhorst pack-grid with 51×1×1 k-points grid. 60×1×1 k-points grid and average 1×10^{-6} eV Fermi level is used.

It is known that phonons are the heat carriers in low-dimensional materials. In a broader sense, phonons in low-dimensional materials can be divided into two groups: low-frequency acoustic phonons and high-frequency optic phonons. More specifically, in-plane longitudinal acoustic (iLA) and in-plane longitudinal optic (iLO) phonons are the main thermal energy transmitters. That is why we have tried to observe the transmission of these phonons. In Fig.2(a), it is found that iLA phonons are transmitted perfectly in pristine ASiNR. It is interesting that instead of atomic vacancy as shown in Fig.2(b), the iLA phonons are transmitted without any attenuation. This incident certifies quantum transport of low-energy phonons. On the other hand, the iLO phonons in Fig.2(c) show that in pristine ASiNR the phonons also transmit easily. But in the vacancy-induced system as shown in Fig.2(d) the iLO phonons are become localized. Only two/three atoms are vibrating. These results are in complete agreement with Refs.[24-36].

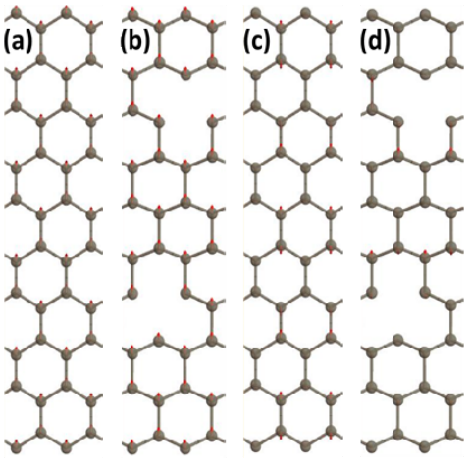

Fig.2 Low-energy iLA phonon (a) without and (b) with vacancies. High-energy iLO phonon (c) without and (d) with vacancies

For more explanation of the above findings, the phonon transmission of the ASiNR is calculated over 0% to 5% atomic vacancies as shown in Fig.3. The effect of 1% and 2% vacancies is not so significant in phonon trans-

mission with 5% vacancy, the phonon transmission decreases about 70% of its pristine condition. The phonon transmission diminishes for the whole range of frequency. Specifically, the inhibition of phonon transmission is greater in the high-frequency region. This is due to the effect of optic phonon localization. Thus, acoustic phonons are fundamental heat carriers in ASiNR.

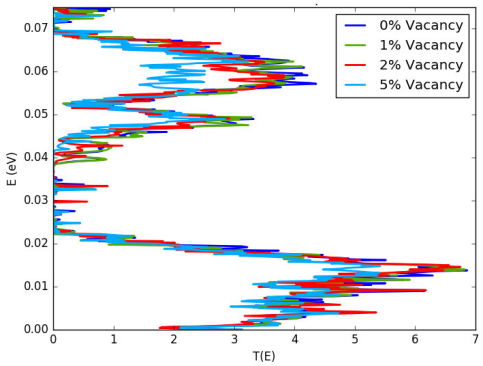

Fig.3 Phonon transmission of (10, 0) ASiNR over 0% to 5% vacancies

Now the PDOSs of ideal (0% vacancy) and non-ideal (1%—5% vacancies) of ASiNR are provided to further investigate the phonon properties, as shown in Fig.4. The PDOS of ideal ASiNR shows all the characteristics peaks corresponding to silicene[37]. The discrete PDOS peaks are called van Hove singularities originated from the one-dimensionality of ASiNR. It is found that with an increasing number of vacancies, both the high- and low-frequency phonons are scattered into other states. The high-frequency phonons tend to shift towards the low-frequency region. The dangling bonds created by the vacancies are the source of this shifting because weakly bonded atoms vibrate with low-frequency. Again, some sharp peaks are observed in the low-frequency region with increasing vacancies.

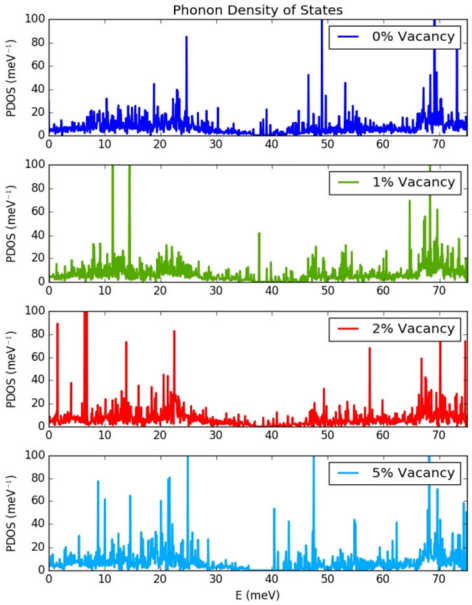

Fig.4 PDOS of ideal and non-ideal AsiNR

The phonon dispersion relation for the whole Brillouin zone is also simulated. From Fig.5(a) and (b) of phonon band structure, it is figured out that, the vacancies create nondegenerate phonon branches (red lines). New branches are created in both low- and high-frequency regions. In pristine case, there are 31 phonon branches and in vacancy defected case the phonon branches raise to 47. Clear evidence of the softening of high-frequency phonon branches is obtained. All the findings give a closer look at the phonons scattering by the atomic vacancies.

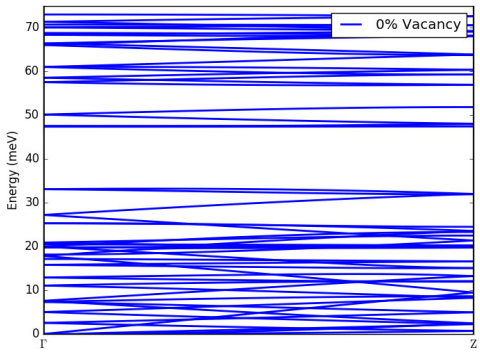

(a) Without vacancy

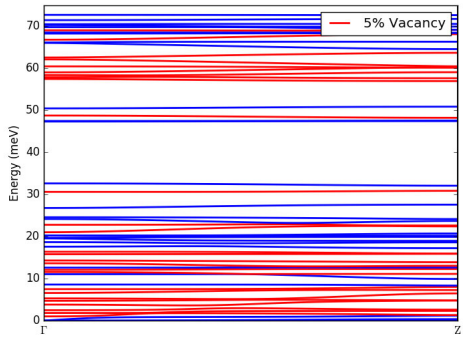

(b) With vacancy

Fig.5 Phonon bandstructures of ASiNR (a) without and (b) with vacancy

The phonon dispersion relation for the whole Brillouin zone is also simulated. From Fig.5(a) and (b) of phonon band structure, it is figured out that, the vacancies create nondegenerate phonon branches (red lines). New branches are created in both low-frequency and high-frequency regions. In pristine case, there are 31 phonon branches and in vacancy defected case the phonon branches raise to 47. Clear evidence of the softening of high-frequency phonon branches is obtained. All the findings give a closer look at the phonons scattering by the atomic vacancies.

The effects of changes in phonon properties ultimately go on phonon thermal conductance. The phonon thermal conductance gradually decreases with increasing vacancies. In the report by Li et al[38], they showed the effects of vacancy defects on phonon thermal conductivity and found significant phonon-defect scattering with the diminution of phonon thermal conductance. Their results showed that phonon transportation in silicene is strongly

affected by atomic vacancy concentrations. Our results in Fig.6 shows that the phonon thermal conductance decreases 30% of pristine condition with 5% vacancies. The phonon thermal conductance increases linearly up to 500 K but the curves tend to saturate beyond this temperature.

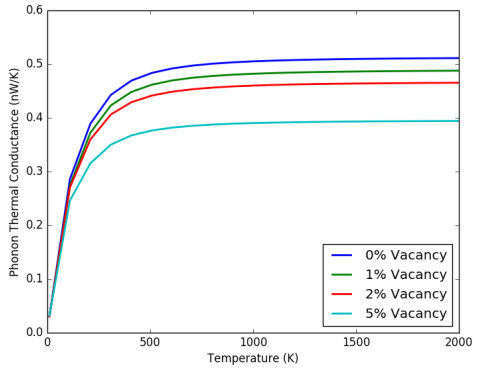

Fig.6 Phonon thermal conductance of ASiNR over 0% to 5% vacancies

In the end, an interesting property called entropy is calculated (Tab.1). The entropy increases almost linearly with respect to vacancies, as entropy reflects the degree of disorder in a system.

Tab.1 Entropy of ASiNR over 0% to 5% vacancies

Vacancy concentration (%)	Entropy (meV/K)
0	54.136 398 068 3
1	54.599 509 445 9
2	55.723 837 468 2
3	57.326 673 245 9
4	59.219 904 673 2
5	63.901 151 653 5

In this letter, an attempt is taken to explore the phonon characteristics of pristine as well as vacancy disordered ASiNR. Various intriguing findings are observed. Among them, quantum transport of acoustic phonon and localization of optic phonon is quite interesting with vacancies. The phonon transmission is suppressed for the whole energy regime. The vacancy effects are much more in the high-energy region than in the low-energy region. The PDOSs indicate the scattering of phonon with atomic vacancies. PDOSs soften towards lower frequency regions due to the creation of dangling bonds with vacancies. Nondegenerate phonon branches are created with the presence of vacancies. The phonon thermal conductance reduces with increasing vacancies. The phonon thermal conductance decreases by about 30% for 5% of vacancy. The interesting property named entropy shows a nearly linear relation with increasing vacancy concentrations. We firmly believe that these findings will be a milestone in developing future SiNR based nanodevices.

References

[1] Y.-L. Song, Y. Zhang, J.-M. Zhang and D.-B. Lu, Applied Surface Science **256**, 6313 (2010).
[2] J. Kang, F. Wu and J. Li, Appl. Phys. Lett. **100**, 233122 (2012).
[3] L. Pan, H. J. Liu, X. J. Tan, H. Y. Lv, J. Shi, X. F. Tang and G. Zheng, Phys. Chem. Chem. Phys. **14**, 13588 (2012).
[4] Y. Jing, Y. Sun, H. Niu and J. Shen, Physica Status Solidi (b) **250**, 1505 (2013).
[5] P. De Padova, O. Kubo, B. Olivieri, C. Quaresima, T. Nakayama, M. Aono and G. Le Lay, Nano Lett. **12**, 5500 (2012).
[6] Y. Wang, J. Zheng, Z. Ni, R. Fei, Q. Liu, R. Quhe, C. Xu, J. Zhou, Z. Gao and J. Lu, Nano **07**, 1250037 (2012).
[7] H. Li, L. Wang, Q. Liu, J. Zheng, W.-N. Mei, Z. Gao, J. Shi and J. Lu, Eur. Phys. J. B **85**, 274 (2012).
[8] M. S. Fahad, A. Srivastava, A. K. Sharma, C. Mayberry and K. M. Mohsin, ECS Trans. **75**, 175 (2016).
[9] B. Aufray, A. Kara, S. Vizzini, H. Oughaddou, C. Léandri, B. Ealet and G. Le Lay, Appl. Phys. Lett. **96**, 183102 (2010).
[10] M. Rachid Tchalala, H. Enriquez, A. J. Mayne, A. Kara, S. Roth, M. G. Silly, A. Bendounan, F. Sirotti, T. Greber, B. Aufray, G. Dujardin, M. Ait Ali and H. Oughaddou, Appl. Phys. Lett. **102**, 083107 (2013).
[11] Y. Ding and J. Ni, Appl. Phys. Lett. **95**, 083115 (2009).
[12] Y.-L. Song, Y. Zhang, J.-M. Zhang, D.-B. Lu and K.-W. Xu, Journal of Molecular Structure **990**, 75 (2011).
[13] L. Ma, J.-M. Zhang, K.-W. Xu and V. Ji, Physica B: Condensed Matter **425**, 66 (2013).
[14] Y. Ding and Y. Wang, Appl. Phys. Lett. **104**, 083111 (2014).
[15] S. M. Aghaei and I. Calizo, in SoutheastCon 2015 (2015), pp. 1–6.
[16] Y . Yao, A. Liu, J. Bai, X. Zhang, and R. Wang, Nanoscale Research Letters **11**, 371 (2016).
[17] D. Zou, W. Zhao, C. Fang, B. Cui, and D. Liu, Phys. Chem. Chem. Phys. **18**, 11513 (2016).
[18] R.-L. An, X.-F. Wang, P. Vasilopoulos, Y.-S. Liu, A.-B. Chen, Y.-J. Dong, and M.-X. Zhai, J. Phys. Chem. C **118**, 21339 (2014).
[19] H. Sadeghi, S. Sangtarash, and C. J. Lambert, Scientific Reports **5**, 09514 (2015).
[20] J.-A. Yan, R. Stein, D. M. Schaefer, X.-Q. Wang, and M. Y. Chou, Phys. Rev. B **88**, 121403 (2013).
[21] E. Scalise, M. Houssa, G. Pourtois, B. van den Broek, V. Afanas'ev, and A. Stesmans, Nano Res. **6**, 19 (2013).
[22] S. Cahangirov, M. Topsakal, E. Aktürk, H. Şahin, and S. Ciraci, Phys. Rev. Lett. **102**, 236804 (2009).
[23] P. Erhart and K. Albe, Phys. Rev. B **71**, 035211 (2005).
[24] A. H. Howlader, M. S. Islam, and A. S. M. J. Islam, 21st International Conference of Computer and Information Technology (ICCIT), 1 (2018).
[25] A. H. Howlader and M. S. Islam, Phonon Transmission

of Vacancy Defected (10,0) Carbon Nanotube, 3rd International Conference on Electrical Information and Communication Technology (EICT), 1 (2017).
[26] K. N. Anindya, M. S. Islam, J. Park, A. G. Bhuiyan and A. Hashimoto, Current Applied Physics **20**, 572 (2020).
[27] Md. S. Islam, A. H. Howlader, K. N. Anindya, R. Zheng, J. Park and A. Hashimoto, Journal of Applied Physics **128**, 045108 (2020).
[28] K. N. Anindya, Md. S. Islam, A. Hashimoto and J. Park, Carbon **168**, 22 (2020).
[29] S. Islam, A. G. Bhuiyan and A. Hashimoto, Realistic edge Shape Effects on The Vibrational Properties of Graphene Nanoribbons, 2nd International Conference on Electrical Information and Communication Technologies (EICT), 412 (2015).
[30] Md. S. Islam, K. Ushida, S. Tanaka and A. Hashimoto, Computational Materials Science **79**, 356 (2013).
[31] Md. S. Islam, K. Ushida, S. Tanaka and A. Hashimoto, Diamond and Related Materials **40**, 115 (2013).
[32] Md. S. Islam, K. Ushida, S. Tanaka, T. Makino and A. Hashimoto, Computational Materials Science **94**, 225 (2014).
[33] Md. S. Islam, K. Ushida, S. Tanaka, T. Makino and A. Hashimoto, Computational Materials Science **94**, 35 (2014).
[34] Md. S. Islam, S. Tanaka and A. Hashimoto, Carbon **80**, 146 (2014).
[35] A. H. Howlader, M. S. Islam, S. Tanaka, T. Makino and A. Hashimoto, Jpn. J. Appl. Phys. **57**, 02CB08 (2018).
[36] M. S. Islam, K. N. Anindya, A. G. Bhuiyan, S. Tanaka, T. Makino and A. Hashimoto, Jpn. J. Appl. Phys. **57**, 02CB04 (2017).
[37] H. Li and R. Zhang, EPL **99**, 36001 (2012).
[38] C . Sevik, H. Sevinçli, G. Cuniberti and T. Çağın, Nano Lett. **11**, 4971 (2011).